A brain atlas of the camouflaging dwarf cuttlefish, *Sepia bandensis*

Tessa G. Montague[1,2,*], Isabelle J. Rieth[1], Sabrina Gjerswold-Selleck[1], Daniella Garcia-Rosales[1], Sukanya Aneja[3], Dana Elkis[3], Nanyan Zhu[1], Sabrina Kentis[1], Frederick A. Rubino[4], Adriana Nemes[1], Katherine Wang[1], Luke A. Hammond[1], Roselis Emiliano[1], Rebecca A. Ober[1], Jia Guo[1], Richard Axel[1,2,*].

[1]The Mortimer B. Zuckerman Mind Brain Behavior Institute, Department of Neuroscience, Columbia University, New York, NY 10027, USA
[2]Howard Hughes Medical Institute, Columbia University, New York, NY 10027, USA
[3]Interactive Telecommunications Program, New York University, New York, NY 10003, USA
[4]Department of Cell Biology, Skirball Institute of Biomolecular Medicine, New York University School of Medicine, New York, NY 10016, USA

*Authors for correspondence

Abstract

The dwarf cuttlefish, *Sepia bandensis*, a small cephalopod that exhibits dynamic camouflage, is an emerging model organism in neuroscience. Coleoid cephalopods (cuttlefish, octopus, and squid) evolved large, complex brains capable of learning, problem-solving, and memory. We used high-resolution magnetic resonance imaging (MRI), deep learning, and fluorescent histology to generate a dwarf cuttlefish brain atlas and built an interactive web tool (cuttlebase.org) to host the data. Guided by observations in other cephalopods, we identified 38 brain lobes. The dwarf cuttlefish brain is partially encased in cartilage and includes two large optic lobes (74% the total volume of the brain), chromatophore lobes whose motor neurons directly innervate the skin, and a vertical lobe that has been implicated in learning and memory. Motor neurons emerging from the chromatophore lobe modulate the color, pattern, and texture of the skin to elicit camouflage. This brain atlas provides a valuable tool for exploring the neural basis of cuttlefish behavior.

Introduction

The coleoid cephalopods are a group of soft-bodied marine mollusks that exhibit an array of interesting biological phenomena, including three hearts, blue blood, color-changing skin, prehensile regenerating

arms, and elaborate motor and social behaviors. In contrast to ancient cephalopods, which possess stereotypical molluskan shells, the coleoid cephalopods internalized or lost these shells over evolutionary time. In addition, they evolved larger brains, camera-type eyes and neurally controlled changes in skin pattern and texture for camouflage and social communication (Amodio et al., 2019; Hanlon & Messenger, 2018). During camouflage, cuttlefish create an approximation of the physical world on their skin. Camouflage is optically driven (Young, 1971; Hanlon & Messenger, 1988) and is a consequence of the activation of motor neurons that project from the brain to radial muscles that surround pigment-filled saccules (chromatophores) of the skin. Excitation elicits an expansion of the chromatophore to reveal pixels of different colors (Messenger, 2001).

The coleoid cephalopod brain surrounds the esophagus and investigators have divided the brain into supra- and subesophageal structures (Dietl, 1878; Hillig, 1912). The supraesophageal structures include a vertical lobe complex involved in learning and memory, and a supraesophageal mass involved in the coordination of motor behaviors. The subesophageal mass comprises multiple motor areas that elicit simpler motor actions (Boycott & Young, 1955; Boycott, 1961; Sanders & Young, 1940). The optic lobe complex, the largest brain structure, resides lateral to the central peri-esophageal structures, and is engaged in visual processing (Young, 1974; Young, 1976; Young, 1977; Young, 1979). The connectivity and function of these structures have been studied by histology (Young, 1971; Young, 1974; Young, 1976; Young, 1977; Young, 1979; Messenger, 1979), tracing (Saidel, 1982; Robertson et al., 1993; Dubas et al., 1986b; Gaston & Tublitz, 2004; Gaston & Tublitz, 2006), lesion (Wells & Young, 1975; Boycott & Young, 1957; Chichery & Chichery, 1987; Fiorito & Chichery, 1995; Messenger, 1967; Graindorge et al., 2006), magnetic resonance imaging (Chung et al., 2020; Chung et al., 2021) and electrophysiology (Chichery & Chanelet, 1976; Boycott, 1961; Dubas et al., 1986a; Bullock & Budelmann, 1991; Zullo et al., 2009; Hochner et al., 2003; Shomrat et al., 2011). Systematic stimulation of individual brain lobes of the European cuttlefish (*Sepia officinalis*) revealed their participation in different motor behaviors, including the movement of the fins, arms and chromatophores (Boycott, 1961). The function of higher processing centers in the supraesophageal mass, however, remain elusive.

The European cuttlefish, *Sepia officinalis,* has been studied most extensively to understand behavior (Hanlon & Messenger, 2018), learning and memory (Turchetti-Maia et al., 2019) and the neural control of skin patterning (Reiter et al., 2018; Hanlon, 2007). We study the dwarf cuttlefish, *Sepia bandensis,* a tropical species from the Indo-Pacific (Figure 1A-D, Video 1). Dwarf cuttlefish are small (<6 cm mantle length), embryonic development is relatively fast (1 month) and they reach sexual maturity in only 4 months (Montague et al., 2021). Dwarf cuttlefish can be bred at relatively high density in the lab, each animal produces dozens of embryos over its lifetime, and the embryos can be cultured *in vitro* to hatching (Montague et al., 2021). These features may permit the introduction of genetically-encoded calcium indicators and light-activated channels that may facilitate an understanding of the relationship between neural activity and behavior.

The study of the neural basis of skin patterning and behavior in the dwarf cuttlefish requires knowledge of its neuroanatomy. Anatomical mapping using histology or MRI has been performed in a small number of octopus and squid species (Chung et al., 2020; Koizumi et al., 2016; Jung et al., 2018; Chung et al., 2021), but a brain atlas has not been generated for any cuttlefish species. In this study, we used high-resolution MRI and deep learning to build a 3D model of the dwarf cuttlefish brain, which we annotated with 38 lobes and nine nerve tracts. In addition, we performed three-plane, whole brain fluorescence histology of the brain, and we used MRI to create an anatomical model of an entire cuttlefish, including the animal's reproductive, digestive, respiratory and circulatory systems. These data allowed us to create an interactive, user-friendly web tool, Cuttlebase (cuttlebase.org).

Results

An MRI-based 3D brain atlas for the dwarf cuttlefish

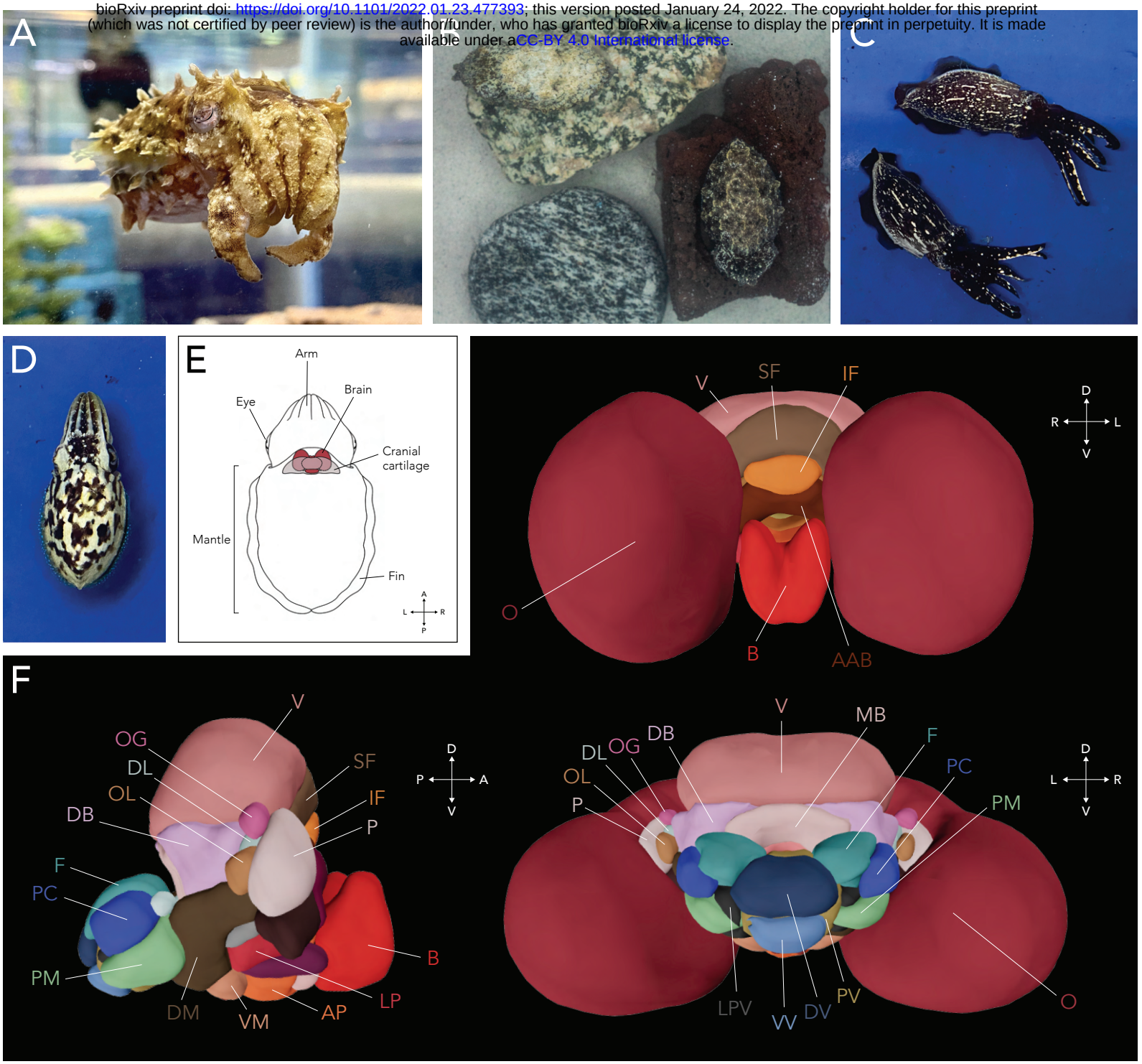

Figure 1. 3D brain atlas of the dwarf cuttlefish, *Sepia bandensis*. A) Adult dwarf cuttlefish (~8 cm in length). B) Cuttlefish camouflage to their surroundings by changing the color and texture of their skin. C) The stereotyped skin pattern and posture assumed by male dwarf cuttlefish during aggressive interactions. D) An innate social skin pattern. E) Anatomy of a cuttlefish. The brain is encased on its posterior side by rigid cartilage. F) 3D template brain, based on MR imaging of 8 brains (4 males, 4 females) and manual annotations of 38 brain lobes and 9 nerve tracts. For abbreviations see Table 1.

The cuttlefish brain is located posterior and medial to the eyes and is encased posteriorly by cranial cartilage (Figure 1E). We performed *ex vivo* magnetic resonance imaging (MRI) of 8 adult dwarf cuttlefish brains (4 males, 4 females) at 50 μm isotropic resolution. Deep learning techniques were applied to extract the brains from their surrounding tissues (see Methods, Figure S1). We used prior neuroanatomical descriptions to guide the annotation of brain lobes (Boycott, 1961; Chung et al., 2020). Finally, we co-registered the 8 brains to create a merged, annotated template brain (Figure 1F). The *ex vivo* dwarf cuttlefish brain is 95% the volume of the *ex vivo* mouse brain (see Methods).

The dwarf cuttlefish brain can be divided into 38 discrete lobes. This value is in accord with previous anatomical studies in other species, but it remains possible that the annotated lobes can be subdivided further. The largest brain lobes, the optic lobes, comprise 74% of the volume of the brain (Table 2) and receive direct projections from the retina. Camouflage is initiated by visual information represented in the optic lobe, which projects directly to the lateral basal lobe (Young, 1962; Boycott, 1961; Young, 1971; Young, 1974). The lateral basal lobe projects to the anterior and posterior chromatophore lobes, which control the chromatophores on the head and arms, and the mantle, respectively (Boycott, 1961; Young, 1976). The posterior chromatophore lobe projects motor neurons to the mantle skin via the pallial nerve, which controls chromatophores and papillae to create skin patterns and three-dimensional texture (Gonzalez-Bellido et al., 2018; Young, 1972; Messenger, 2001; Boycott, 1961). We have focused on the flow of information thought to elicit skin patterning, but the atlas provides information on the brain regions involved in several additional behaviors (Table 1) (Nixon & Young, 2003; Hanlon & Messenger, 2018).

A histological brain atlas for the dwarf cuttlefish

We complemented the anatomical description of the cuttlefish brain with histological examination of the entire brain to obtain cellular resolution. We sectioned the brain in the transverse, horizontal and sagittal planes (Figure 2A). All sections were stained with Phalloidin, an F-actin peptide that labels axons, and

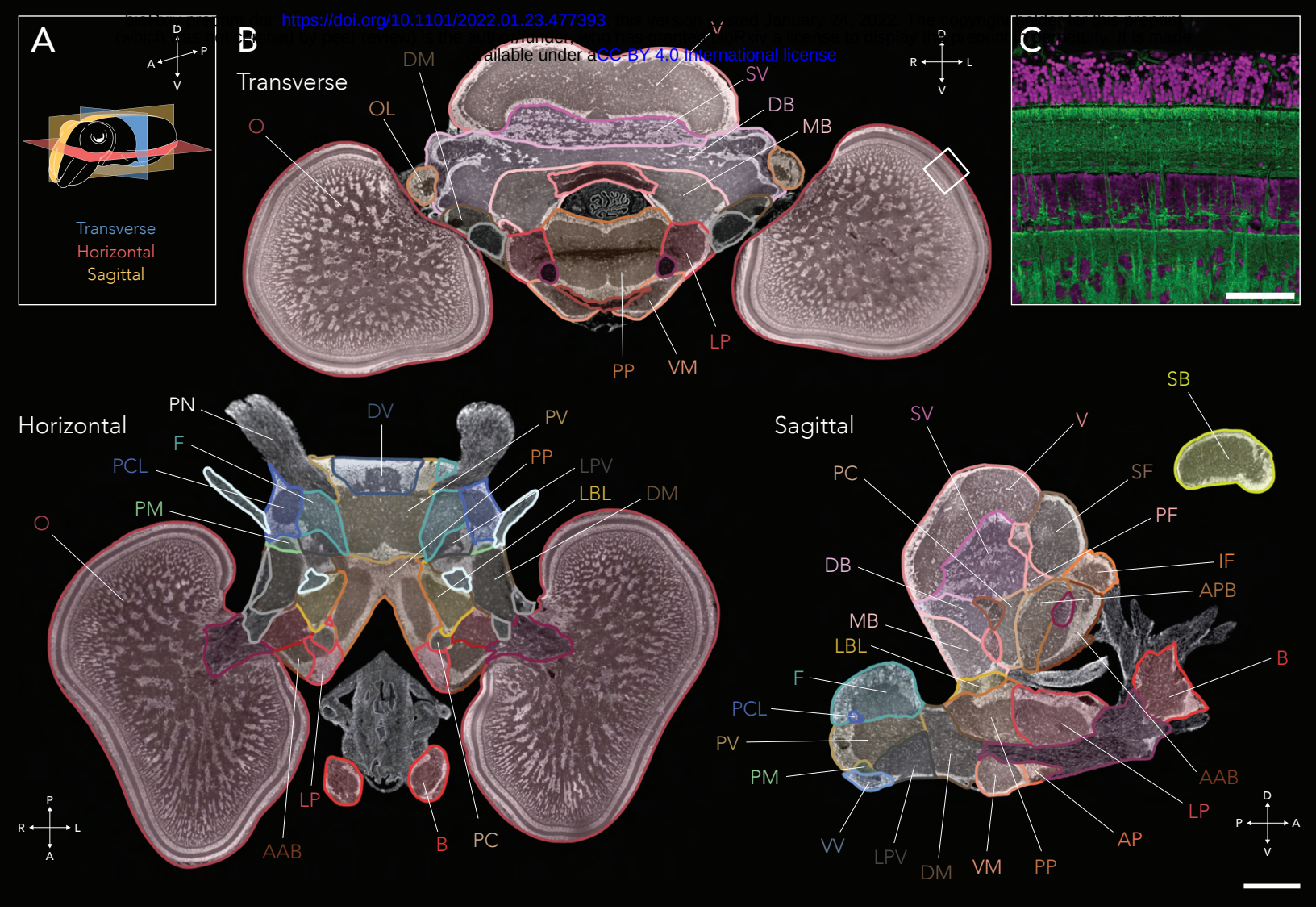

Figure 2. Histological brain atlas of the dwarf cuttlefish, *Sepia bandensis*. A) The cuttlefish brain can be sectioned in the transverse, horizontal and sagittal planes. B) Histological slices of the cuttlefish brain stained with NeuroTrace, a Nissl stain that labels cell bodies, and annotated with 38 brain lobes and 9 nerve tracts. Scale bar, 1 mm. For abbreviations see Table 1. C) Confocal image of the layered cortex of the optic lobe (white square in Figure 2B). Scale bar, 100 µm.

NeuroTrace, a Nissl stain that labels cell bodies. Our annotated 3D MRI datasets and a prior neuroanatomical description (Boycott, 1961) were used to describe the histological organization of 38 brain lobes and 9 nerve tracts (Figure 2B). Phalloidin and NeuroTrace staining confirmed organizational features of the cephalopod brain. The majority of lobes are discrete and bounded, a feature not uniformly observed in vertebrate brains. Each lobe contains an outer perikaryal layer of cell bodies that surrounds a dense, inner neuropil (Figure 2B). The optic lobe is comprised of a layered cortex, with two cell layers apposing a plexiform zone of fibers (Young, 1962; Young, 1974) (Figure 2C) and a central medulla with cell islands that are connected in a tree-like structure (Liu et al., 2017; Young, 1962; Young, 1974). The two outer layers may share properties with the lamina and medulla of dipteran optic lobes (Shinomiya et al., 2019).

Cuttlebase - a web tool for visualizing the cuttlefish brain

We built an interactive web tool to maximize the utility of our brain atlas (Figure 3A). Cuttlebase features multiple tools for the dwarf cuttlefish, including 3D models of the adult cuttlefish brain (Figure 3B) and body (Figure 3C), as well as annotated histological sections of the brain in 3 planes (Figure 3A). We visualized the cranial cartilage — the only rigid tissue around the brain — in the 3D and histological atlas to facilitate the development of methods to head-fix cuttlefish, an important step for stabilizing the brain for two-photon imaging or electrophysiology. Cuttlebase is easy-to-use, with an array of features designed for both novice and expert users, including responsive, color-coded labels for each brain region, the ability to zoom, rotate and screenshot the data, synchronized graphics that denote the brain's orientation, and options to show the brain's position within the cuttlefish body.

Discussion

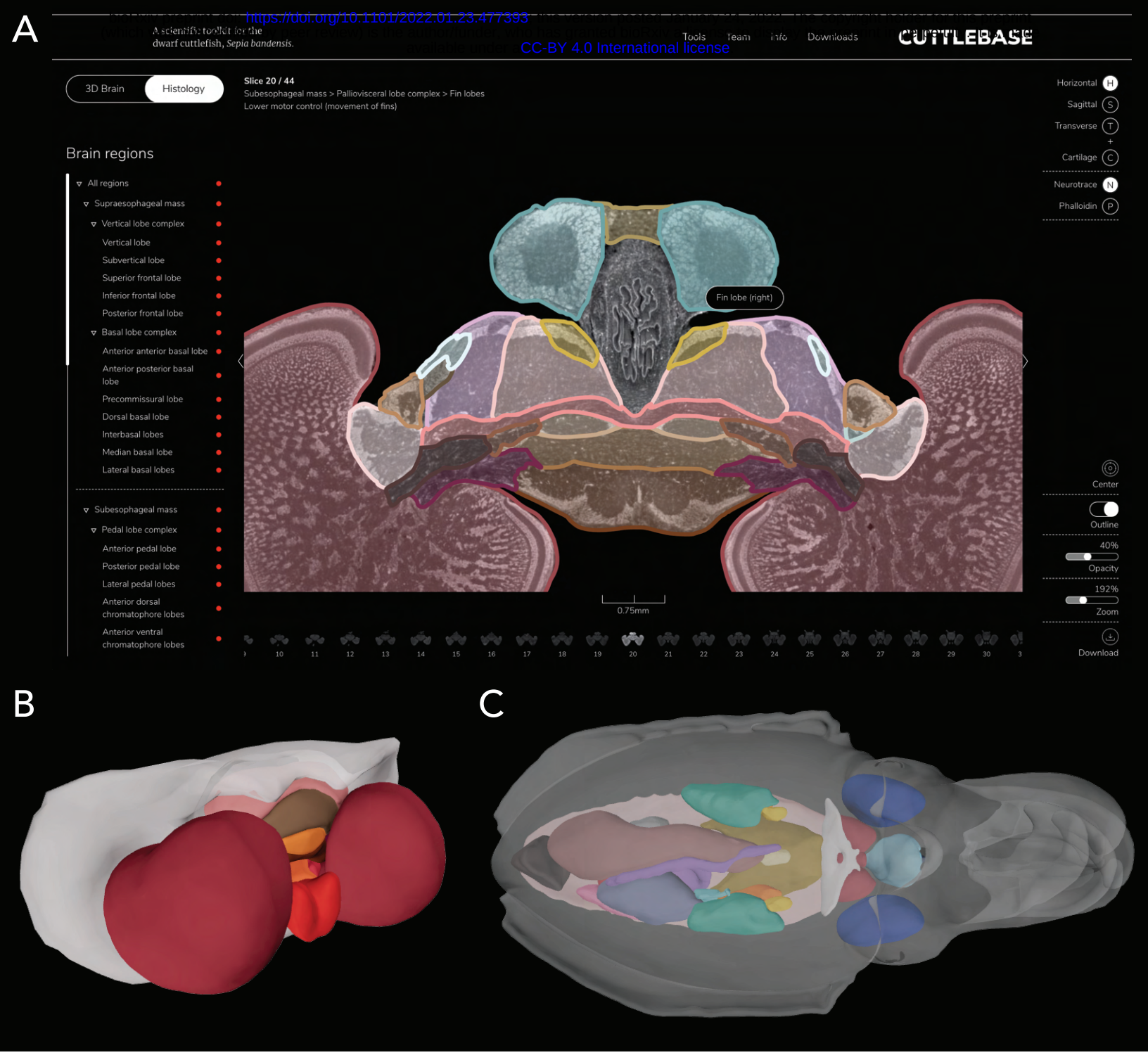

Figure 3. Cuttlebase is a scientific toolkit for the dwarf cuttlefish. A) Cuttlebase hosts multiple dwarf cuttlefish tools including an interactive brain atlas, which features color-coded and responsive labels, and the ability to screenshot, zoom and rotate the data. B) The 3D brain can be visualized with the cranial cartilage. C) Cuttlebase also hosts a body atlas, labeled with 21 organs and tissues.

The brain of the dwarf cuttlefish exhibits structural similarities with other decapodiformes, the 10-armed cuttlefish and squid, but is somewhat different from the brain of octopodiformes, octopus and vampire squid (Albertin & Simakov, 2020). First, the decapodiformes, but not octopodiformes, possess a giant-fiber system, which is used for funnel-based jet propulsion during escape behaviors. The giant cells are located in the ventral magnocellular lobe, and receive input from the optic lobes and statocysts (the cephalopod vestibular system) (Nixon & Young, 2003; Abbott et al., 1995). Second, the brachial, pedal and inferior frontal lobes of octopus are larger than the decapodiformes, which may facilitate their more sophisticated use of arms and tactile learning (Ponte et al., 2020). Third, the octopus vertical lobe is folded into gyri, creating a larger surface area (Young, 1971). Finally, the decapodiformes, but not octopodiformes, possess a fin lobe, used for fin locomotion (Boycott, 1961). Most decapodiformes use two forms of locomotion: jet propulsion using the funnel, and swimming using the funnel and fins (Russell & Steven, 1930). Interestingly, the dwarf cuttlefish uses an additional mode: it can walk bipedally using its ventral arms (Video 2). This may require the evolution of a control system for coordinated locomotion.

Analysis of the dwarf cuttlefish brain atlas reveals notable differences between the brains of the coleoid cephalopods (octopus, cuttlefish and squid) and the nautilus, a living order of an otherwise extinct lineage (Crook & Basil, 2008). Unlike the large, centralized brains of the coleoid cephalopods, the nautilus central nervous system features 3 simple nerve cords with minimal subdivisions. The nautilus brain does not appear to contain the motor areas for the elaborate control of limbs, nor the higher brain areas for learning and memory (Young, 1965; Budelmann, 1995). Nautiluses have pinhole eyes (Muntz & Raj, 1984) and smaller optic lobes (Young, 1965). However, the olfactory lobes of nautiluses are much larger than that of the coleoid cephalopods (Young, 1965), consistent with the central role of olfaction in nautilus foraging (Basil et al., 2000).

The dwarf cuttlefish brain atlas presented here serves multiple functions. First, the MRI-based 3D brain model affords users the ability to locate specific targets for electrophysiological recordings or calcium

imaging experiments of neural activity. Second, the histological atlas facilitates the identification of brain regions in anterograde and retrograde tracing experiments. Third, the neuroanatomical and histological atlases facilitate the identification of regionally-restricted genes that may provide specificity to efforts at genetic manipulation. Fourth, the entire dataset is a comprehensive resource for comparative neuroanatomical analyses. Finally, the addition of a cuttlefish body atlas allows users to see the physiological context of the brain and may permit the study of communication between the brain and internal organs. The generation of the neuroanatomical and histological atlas for the dwarf cuttlefish may inform studies in other cephalopods, for which atlases do not exist, and now renders *Sepia bandensis* a more facile system for the study of the neural control of camouflage.

Materials & Methods

3D brain atlas

MRI acquisition

8 adult cuttlefish (4 male, 4 female) were euthanized in 10% ethanol, and the brain and connected eyes were surgically removed and fixed overnight in a solution of 4% paraformaldehyde (PFA) in filtered artificial seawater (FASW) at 4°C. The fixed brains were washed in PBS, incubated in 0.2% OMNISCAN (gadodiamide) for 2 days at 4°C to increase contrast, and then suspended in fomblin in a 15 mL conical tube. Imaging was performed on a Bruker BioSpec 94/30 horizontal small animal MRI scanner (field strength, 9.4 T; bore size, 30 cm) equipped with a CryoProbe and ParaVision 6.0.1 software (Bruker). A 23 mm 1H circularly polarized transmit/receive-capable mouse head volume coil was used for imaging. For each cuttlefish, one scan was acquired of the brain and eyes (to obtain a scan of the entire cranial cartilage), and a higher resolution scan was acquired of the brain only. T1-weighted images were acquired with a Fast Low Angle Shot (FLASH) sequence (brain/eye scan: TR = 50 ms, TE = 10 ms, FOV = 30 x 24 x

15 mm^3, voxel size = 100 x 100 x 100 μm^3, scan time = 33 m 12 s; brain-only scan: TR = 50 ms, TE = 8.5 ms, FOV = 14 x 12 x 11 mm^3, voxel size = 60 x 60 x 60 μm^3, scan time = 4 hr 28 m).

MRI processing & brain extraction

All scans underwent N4 bias field correction (Tustison et al., 2010). Whole brain scans were isotropically upsampled to 50 μm isotropic resolution with cubic B-spline interpolation. To computationally extract the brains from their surrounding tissue, brain masks were generated by an in-house deep learning model (Gjerswold-Selleck et al., 2021), which was pre-trained with brain masks manually annotated in 3D Slicer (Fedorov et al., 2012). The deep learning brain masks were manually polished using the 3D Slicer Segment Editor and then used to extract the brain from each brain-only MRI scan ("brain-extracted images") (Figure S1). For the brain/eye scans, the cranial cartilage was manually segmented in 3D Slicer using the Segment Editor. The cartilage masks were used to extract the cartilage from each brain/eye MRI scan ("cartilage-extracted images").

Segmentation

Two of the whole brain scans (1 male, 1 female) were manually segmented in 3D Slicer by 6 independent annotators guided by prior neuroanatomical descriptions (Boycott, 1961; Chung et al., 2020). The brain label maps for each subject were merged using pixel-level majority voting, transformed to the remaining 6 subjects, and then manually corrected, resulting in 8 brain label maps corresponding to the 8 subjects.

Generation of the template brain

The final MRI atlas was built by merging the brain template, built from the high-resolution brain-only scans with the cranial cartilage template, built from the brain/eye scans. First, to generate each template, a population average of brain-extracted or cartilage-extracted images was constructed through an iterative process by averaging the co-registered images over multiple cycles using a symmetric diffeomorphic algorithm with cubic-spline interpolation (Avants et al., 2011). The brain label map (annotations) for each subject was diffeomorphically transformed to the whole brain template space and combined through pixel-

level majority voting. The brain/eye template was isotropically upsampled to match the 50 µm resolution of the whole brain scans, and the whole brain template underwent rigid registration to align it with the brain/eye template. Finally, the brain regions of the whole brain template were combined with the cartilage regions of the whole head template to build a single atlas. In the regions where the two templates overlapped, pixel values of the high-resolution whole brain template were selected. The cuttlefish brain label map was smoothed by taking a majority vote in a local neighborhood with a 3 x 3 x 3 kernel size.

Brain volume calculation

A mouse MRI brain model (15 µm resolution, average of 18 *ex vivo* subjects) was downloaded from the Australian Mouse Brain Mapping Consortium (nonsymmetric version, NiFTI format, https://imaging.org.au/AMBMC/Model), and then downsampled to 50 µm resolution and imported into 3D Slicer. Using the Editor tool at a threshold of zero, a mask was generated of the entire mouse brain, and the spinal cord was manually removed using the eraser tool. The volume of the mouse brain mask was calculated using the Label Statistics tool (total volume: 332.7 mm^3). To calculate the volume of the cuttlefish brain, the volume of each brain lobe in the merged, template brain was calculated using the Label Statistics tool and summed (total volume: 313.7 mm^3), see Table 2.

Histological atlas

Adult cuttlefish were euthanized in 10% ethanol, and the brain and connected eyes were surgically removed and fixed overnight in a solution of 4% paraformaldehyde (PFA) in filtered artificial seawater (FASW) at 4°C. Note that fixing brains in a solution of PBS (instead of FASW) created abnormal cell morphologies. The fixed brains were washed in PBS, the eyes were removed with a scalpel, and the brains were incubated in 10% sucrose overnight followed by 30% sucrose overnight at 4°C. The brains were embedded in OCT on dry ice and stored at -80°C. Each brain was sliced in 100 µm sections on a cryostat (Leica CM3050 S), and the sections were dried overnight at room temperature. The sections were stained with Phalloidin (Life Technologies #A12379, 1/40 dilution) and NeuroTrace (Life

Technologies #N21482, 1/20 dilution) and then imaged on a custom-built Nikon AZ100 Multizoom Slide Scanner. Images were registered using BrainJ (http://github.com/lahammond/BrainJ). Brightness and contrast were adjusted uniformly across each image, and surrounding tissue was removed manually from the image in FIJI and Photoshop. The data was manually segmented in 3D Slicer by two annotators using a neuroanatomical study (Boycott, 1961) and our 3D brain atlas for reference.

Whole body atlas

An adult male cuttlefish was anesthetized in $MgCl_2$ (17.5g/L) and then euthanized in 10% ethanol, fixed for 2 days in 4% PFA/FASW at 4°C, and then transferred to 0.2% OMNISCAN (gadodiamide) for 2 days at 4°C to increase contrast. The fixed specimen was suspended in fomblin in a custom-made vessel and imaged on a Bruker BioSpec 94/30 horizontal small animal MRI scanner (field strength, 9.4 T; bore size, 30 cm) equipped with a CryoProbe and ParaVision 6.0.1 software (Bruker). A 112/86-mm 1H circularly polarized transmit/receive-capable volume coil was used for imaging. T1-weighted images were acquired with a FLASH sequence (TR = 55 ms, TE = 17 ms, FOV = 90 x 48 x 38 mm^3, voxel size = 100 x 100 x 100 μm^3, scan time = 2 hr 47 m). The scan underwent N4 bias field correction (Tustison et al., 2010) and was manually segmented in 3D Slicer using anatomical descriptions (Gestal et al., 2019).

Cuttlebase

The Cuttlebase web content is delivered using React, a Javascript front-end framework for dynamic websites. React-three-fiber (a Three.js wrapper for React) is used to assist with interactions in the 3D view.

3D brain

In 3D Slicer, each segment (brain lobe or tract) of the final, template brain was exported as an STL file and then labelled with a unique identifier in Blender, a 3D authoring software. The 3D model was

277 exported as a GLB, and then imported into a webpage using Three.js - a Javascript library for handling
278 3D content on the web. A custom web-interface was created to assign colors to each of the region
279 meshes, and this data was exported as a JSON file.
280
281 **Histology**
282 To convert the histological annotations to high-resolution images that could be toggled on Cuttlebase,
283 each segment (brain lobe or tract) for each brain (horizontal, sagittal and transverse) was converted to a
284 binary label map in 3D Slicer and saved as a TIFF stack. Each TIFF stack was resized to the canvas size
285 of the original image in Fiji (Schindelin et al., 2012), and saved as a JPEG Stack in monochrome. The
286 images were then inverted and processed with Potrace (through a custom Node.js script), to create
287 SVGs for each region of each layer. The SVGs for all regions in a single layer were combined, and each
288 region was assigned the color corresponding to the 3D atlas. These images, along with the originals,
289 were resized and cropped for more efficient web delivery. Additionally, the cartilage in each Phalloidin
290 section was isolated (by outlining) using Adobe Illustrator, and exported as a PNG. These images were
291 used as masks on the NeuroTrace layers with the command-line tool ImageMagick, to automate this
292 process for the remaining images. Custom Bash scripts were used to manage and organize the large
293 amounts of data and the processing steps required.
294
295 **Data availability**
296
297 All data generated in this study is available to download from cuttlebase.org/downloads.
298
299 **Acknowledgements**
300
301 We wish to thank Connor Gibbons, Sonia Thomas, Telicia Lewis, Sarah Wilson and Josh Barber for
302 cuttlefish care, the Zuckerman Institute Cellular Imaging platform for instrument use and technical
303 support and Lokke Highstein for IT support. This project was funded by a Zuckerman Institute MRI Seed

Grant (T.G.M. and R.A.), the Howard Hughes Medical Institute Hanna H. Gray Fellowship (T.G.M.), the Zuckerman Institute BRAINYAC Program (R.E.) and the Howard Hughes Medical Institute (R.A.)

Competing interests

The authors have no competing interests.

Rich media file legends

Video 1. Dwarf cuttlefish produce waves (of unknown function) on their skin.

Video 2. Dwarf cuttlefish can walk bipedally using their ventral arms.

References

Abbott, N. J., Williamson, R., & Maddock, L. (1995). Cephalopod Neurobiology. Oxford University Press, USA. http://books.google.com/books?id=r1MXAQAAIAAJ&hl=&source=gbs_api

Albertin, C. B., & Simakov, O. (2020). Cephalopod Biology: At the Intersection Between Genomic and Organismal Novelties. Annu Rev Anim Biosci, 8, 71-90. https://doi.org/10.1146/annurev-animal-021419-083609

Amodio, P., Boeckle, M., Schnell, A. K., Ostojíc, L., Fiorito, G., & Clayton, N. S. (2019). Grow Smart and Die Young: Why Did Cephalopods Evolve Intelligence. Trends Ecol Evol, 34(1), 45-56. https://doi.org/10.1016/j.tree.2018.10.010

Avants, B. B., Tustison, N. J., Song, G., Cook, P. A., Klein, A., & Gee, J. C. (2011). A reproducible evaluation of ANTs similarity metric performance in brain image registration. Neuroimage, 54(3), 2033-2044. https://doi.org/10.1016/j.neuroimage.2010.09.025

Basil, J. A., Hanlon, R. T., Sheikh, S. I., & Atema, J. (2000). Three-dimensional odor tracking by Nautilus pompilius. J Exp Biol, 203(Pt 9), 1409-1414. https://pubmed.ncbi.nlm.nih.gov/10751156

Boycott, B. B. (1961). The functional organization of the brain of the cuttlefish Sepia officinalis. Proceedings of the Royal Society of London. Series B, Biological Sciences, 153, 503-534.

Boycott, B. B., & Young, J. Z. (1957). Effects of interference with the vertical lobe on visual discriminations in Octopus vulgaris Lamarck. Proc R Soc Lond B Biol Sci, 146(925), 439-459. https://doi.org/10.1098/rspb.1957.0023

Boycott, B. B., & Young, J. Z. (1955). A memory system in Octopus vulgaris Lamarck. Proc R Soc Lond B Biol Sci, 143(913), 449-480. https://doi.org/10.1098/rspb.1955.0024

Budelmann, B. U. (1995). The cephalopod nervous system: what evolution has made of the molluscan design. In The nervous systems of invertebrates: An evolutionary and comparative approach (pp. 115-138). Springer. https://link.springer.com/chapter/10.1007/978-3-0348-9219-3_7

342 Bullock, T. H., & Budelmann, B. U. (1991). Sensory evoked potentials in unanesthetized unrestrained
343 cuttlefish: a new preparation for brain physiology in cephalopods. J Comp Physiol A, 168(1), 141-150.
344 https://doi.org/10.1007/BF00217112
345 Chichery, M. P., & Chichery, R. (1987). The anterior basal lobe and control of prey-capture in the
346 cuttlefish (Sepia officinalis). Physiol Behav, 40(3), 329-336. https://doi.org/10.1016/0031-9384(87)90055-
347 2
348 Chichery, R., & Chanelet, J. (1976). Motor and behavioral responses obtained by stimulation with chronic
349 electrodes of the optic lobe of Sepia officinalis. Brain Res, 105(3), 525-532.
350 https://doi.org/10.1016/0006-8993(76)90598-9
351 Chung, W. S., Kurniawan, N. D., & Marshall, N. J. (2020). Toward an MRI-Based Mesoscale Connectome
352 of the Squid Brain. iScience, 23(1), 100816. https://doi.org/10.1016/j.isci.2019.100816
353 Chung, W. S., Kurniawan, N. D., & Marshall, N. J. (2021). Comparative brain structure and visual
354 processing in octopus from different habitats. Curr Biol, S0960-9822(21)01532.
355 https://doi.org/10.1016/j.cub.2021.10.070
356 Crook, R. J., & Basil, J. A. (2008). A role for nautilus in studies of the evolution of brain and behavior.
357 Commun Integr Biol, 1(1), 18-19. https://doi.org/10.4161/cib.1.1.6465
358 Dietl, M. J. (1878). Untersuchungen über die Organisation des Gehirns wirbelloser Thiere
359 (Cephalopoden, Tethys). Sitzungsberichte der Akademie der Wissenschaften in Wien, 77, 481-533.
360 Dubas, F., Hanlon, R. T., Ferguson, G. P., & Pinsker, H. M. (1986a). Localization and stimulation of
361 chromatophore motoneurones in the brain of the squid, Lolliguncula brevis. J Exp Biol, 121, 1-25.
362 https://pubmed.ncbi.nlm.nih.gov/3958673
363 Dubas, F., Leonard, R. B., & Hanlon, R. T. (1986b). Chromatophore motoneurons in the brain of the
364 squid, Lolliguncula brevis: an HRP study. Brain Res, 374(1), 21-29. https://doi.org/10.1016/0006-
365 8993(86)90390-2
366 Fedorov, A., Beichel, R., Kalpathy-Cramer, J., Finet, J., Fillion-Robin, J. C., Pujol, S., Bauer, C.,
367 Jennings, D., Fennessy, F., Sonka, M., Buatti, J., Aylward, S., Miller, J. V., Pieper, S., & Kikinis, R. (2012).
368 3D Slicer as an image computing platform for the Quantitative Imaging Network. Magn Reson Imaging,
369 30(9), 1323-1341. https://doi.org/10.1016/j.mri.2012.05.001
370 Fiorito, G., & Chichery, R. (1995). Lesions of the vertical lobe impair visual discrimination learning by
371 observation in Octopus vulgaris. Neurosci Lett, 192(2), 117-120. https://doi.org/10.1016/0304-
372 3940(95)11631-6
373 Gaston, M. R., & Tublitz, N. J. (2004). Peripheral innervation patterns and central distribution of fin
374 chromatophore motoneurons in the cuttlefish Sepia officinalis. J Exp Biol, 207(Pt 17), 3089-3098.
375 https://doi.org/10.1242/jeb.01145
376 Gaston, M. R., & Tublitz, N. J. (2006). Central distribution and three-dimensional arrangement of fin
377 chromatophore motoneurons in the cuttlefish Sepia officinalis. Invert Neurosci, 6(2), 81-93.
378 https://doi.org/10.1007/s10158-006-0021-3
379 Gestal, C., Pascual, S., Guerra, Á., Fiorito, G., & Vieites, J. M. (2019). Handbook of Pathogens and
380 Diseases in Cephalopods. Springer.
381 https://play.google.com/store/books/details?id=aEaMDwAAQBAJ&source=gbs_api
382 Gjerswold-Selleck, S., Zhu, N., Sun, H., Sikka, D., Shi, J., Liu, C., Nuriel, T., Small, S. A., & Guo, J.
383 (2021). DL-BET-A deep learning based tool for automatic brain extraction from structural magnetic
384 resonance images in mice. In.
385 Gonzalez-Bellido, P. T., Scaros, A. T., Hanlon, R. T., & Wardill, T. J. (2018). Neural control of dynamic 3-
386 dimensional skin papillae for cuttlefish camouflage. iScience, 1, 24-34. https://doi.org/10.1016/j.isci
387 Graindorge, N., Alves, C., Darmaillacq, A. S., Chichery, R., Dickel, L., & Bellanger, C. (2006). Effects of
388 dorsal and ventral vertical lobe electrolytic lesions on spatial learning and locomotor activity in Sepia
389 officinalis. Behav Neurosci, 120(5), 1151-1158. https://doi.org/10.1037/0735-7044.120.5.1151
390 Hanlon, R. (2007). Cephalopod dynamic camouflage. Curr Biol, 17(11), R400-4.
391 https://doi.org/10.1016/j.cub.2007.03.034
392 Hanlon, R. T., & Messenger, J. B. (1988). Adaptive coloration in young cuttlefish (Sepia officinalis L.): the
393 morphology and development of body patterns and their relation to behaviour. Philosophical
394 Transactions of the Royal Society of London. B, Biological Sciences, 320(1200), 437-487.
395 https://royalsocietypublishing.org/doi/abs/10.1098/rstb.1988.0087

Hanlon, R. T., & Messenger, J. B. (2018). Cephalopod behaviour. Cambridge University Press. https://books.google.com/books?hl=en&lr=&id=oppPDwAAQBAJ&oi=fnd&pg=PR11&dq=cephalopod+behaviour+messenger&ots=C-2bL6f2Gz&sig=-X_Wre4oCEhgA7Uwv95f8gNiNCE

Hillig, R. (1912). Das Nervensystem von Sepia officinalis L. Z. wiss. Zoo, 101, 736-800.

Hochner, B., Brown, E. R., Langella, M., Shomrat, T., & Fiorito, G. (2003). A learning and memory area in the octopus brain manifests a vertebrate-like long-term potentiation. J Neurophysiol, 90(5), 3547-3554. https://doi.org/10.1152/jn.00645.2003

Jung, S.-H., Song, H. Y., Hyun, Y. S., Kim, Y.-C., Whang, I., Choi, T.-Y., & Jo, S. (2018). A brain atlas of the long arm octopus, octopus minor. Experimental neurobiology, 27(4), 257. https://www.ncbi.nlm.nih.gov/pmc/articles/PMC6120969

Koizumi, M., Shigeno, S., Mizunami, M., & Tanaka, N. K. (2016). Three-dimensional brain atlas of pygmy squid, Idiosepius paradoxus, revealing the largest relative vertical lobe system volume among the cephalopods. J Comp Neurol, 524(10), 2142-2157. https://doi.org/10.1002/cne.23939

Liu, Y. C., Liu, T. H., Su, C. H., & Chiao, C. C. (2017). Neural Organization of the Optic Lobe Changes Steadily from Late Embryonic Stage to Adulthood in Cuttlefish Sepia pharaonis. Front Physiol, 8, 538. https://doi.org/10.3389/fphys.2017.00538

Messenger, J. B. (1967). The effects on locomotion of lesions to the visuo-motor system in octopus. Proceedings of the Royal Society of London. Series B. Biological Sciences, 167(1008), 252-281. https://royalsocietypublishing.org/doi/abs/10.1098/rspb.1967.0026

Messenger, J. B. (1979). The nervous system of Loligo IV. The peduncle and olfactory lobes. Philosophical Transactions of the Royal Society of London. B, Biological Sciences, 285(1008), 275-309. https://royalsocietypublishing.org/doi/abs/10.1098/rstb.1979.0007

Messenger, J. B. (2001). Cephalopod chromatophores: neurobiology and natural history. Biol Rev Camb Philos Soc, 76(4), 473-528. https://doi.org/10.1017/s1464793101005772

Montague, T. G., Rieth, I. J., & Axel, R. (2021). Embryonic development of the camouflaging dwarf cuttlefish, Sepia bandensis. Dev Dyn. https://doi.org/10.1002/dvdy.375

Muntz, W. R. A., & Raj, U. (1984). On the visual system of Nautilus pompilius. Journal of Experimental Biology, 109(1), 253-263. https://journals.biologists.com/jeb/article-abstract/109/1/253/4173

Nixon, M., & Young, J. Z. (2003). The Brains and Lives of Cephalopods. Oxford University Press. http://books.google.com/books?id=BRvrtsuKc6MC&hl=&source=gbs_api

Ponte, G., Taite, M., Borrelli, L., Tarallo, A., Allcock, A. L., & Fiorito, G. (2020). Cerebrotypes in Cephalopods: Brain Diversity and Its Correlation With Species Habits, Life History, and Physiological Adaptations. Front Neuroanat, 14, 565109. https://doi.org/10.3389/fnana.2020.565109

Reiter, S., Hülsdunk, P., Woo, T., Lauterbach, M. A., Eberle, J. S., Akay, L. A., Longo, A., Meier-Credo, J., Kretschmer, F., Langer, J. D., Kaschube, M., & Laurent, G. (2018). Elucidating the control and development of skin patterning in cuttlefish. Nature, 562(7727), 361-366. https://doi.org/10.1038/s41586-018-0591-3

Robertson, J. D., Schwartz, O. M., & Lee, P. (1993). Carbocyanine dye labeling reveals a new motor nucleus in octopus brain. J Comp Neurol, 328(4), 485-500. https://doi.org/10.1002/cne.903280404

Russell, F. S., & Steven, G. A. (1930). The swimming of cuttlefish. Nature, 125(3163), 893-893. https://www.nature.com/articles/125893a0

Saidel, W. M. (1982). Connections of the octopus optic lobe: an HRP study. J Comp Neurol, 206(4), 346-358. https://doi.org/10.1002/cne.902060403

Sanders, F. K., & Young, J. Z. (1940). Learning and other functions of the higher nervous centres of Sepia. Journal of Neurophysiology, 3(6), 501-526. https://journals.physiology.org/doi/pdf/10.1152/jn.1940.3.6.501

Schindelin, J., Arganda-Carreras, I., Frise, E., Kaynig, V., Longair, M., Pietzsch, T., Preibisch, S., Rueden, C., Saalfeld, S., Schmid, B., Tinevez, J. Y., White, D. J., Hartenstein, V., Eliceiri, K., Tomancak, P., & Cardona, A. (2012). Fiji: an open-source platform for biological-image analysis. Nat Methods, 9(7), 676-682. https://doi.org/10.1038/nmeth.2019

Shinomiya, K., Horne, J. A., McLin, S., Wiederman, M., Nern, A., Plaza, S. M., & Meinertzhagen, I. A. (2019). The Organization of the Second Optic Chiasm of the Drosophila Optic Lobe. Front Neural Circuits, 13, 65. https://doi.org/10.3389/fncir.2019.00065

449 Shomrat, T., Graindorge, N., Bellanger, C., Fiorito, G., Loewenstein, Y., & Hochner, B. (2011). Alternative
450 sites of synaptic plasticity in two homologous “fan-out fan-in” learning and memory networks. Curr Biol,
451 21, 1773-1782. https://doi.org/10.1016/j.cub.2011.09.011
452 Turchetti-Maia, A., Shomrat, T., & Hochner, B. (2019). The Vertical Lobe of Cephalopods., 558-574.
453 https://doi.org/10.1093/oxfordhb/9780190456757.013.29
454 Tustison, N. J., Avants, B. B., Cook, P. A., Zheng, Y., Egan, A., Yushkevich, P. A., & Gee, J. C. (2010).
455 N4ITK: improved N3 bias correction. IEEE Trans Med Imaging, 29(6), 1310-1320.
456 https://doi.org/10.1109/TMI.2010.2046908
457 Wells, M. J., & Young, J. Z. (1975). The subfrontal lobe and touch learning in the octopus. Brain Res,
458 92(1), 103-121. https://doi.org/10.1016/0006-8993(75)90530-2
459 Young, J. Z. (1962). The optic lobes of Octopus vulgaris. Philosophical Transactions of the Royal Society
460 of London. Series B, Biological Sciences, 245(718), 19-58.
461 https://royalsocietypublishing.org/doi/pdf/10.1098/rstb.1962.0005
462 Young, J. Z. (1965). The central nervous system of Nautilus. Philosophical Transactions of the Royal
463 Society of London. Series B, Biological Sciences, 249(754), 1-25.
464 https://royalsocietypublishing.org/doi/abs/10.1098/rstb.1965.0006
465 Young, J. Z. (1971). The Anatomy of the Nervous System of Octopus Vulgaris. Oxford University Press,
466 USA. http://books.google.com/books?id=rRUWAQAAIAAJ&hl=&source=gbs_api
467 Young, J. Z. (1972). The organization of a cephalopod ganglion. Philos Trans R Soc Lond B Biol Sci,
468 263(854), 409-429. https://doi.org/10.1098/rstb.1972.0005
469 Young, J. Z. (1974). The central nervous system of Loligo. I. The optic lobe. Philos Trans R Soc Lond B
470 Biol Sci, 267(885), 263-302. https://doi.org/10.1098/rstb.1974.0002
471 Young, J. Z. (1976). The nervous system of Loligo. II. Suboesophageal centres. Philos Trans R Soc Lond
472 B Biol Sci, 274(930), 101-167. https://doi.org/10.1098/rstb.1976.0041
473 Young, J. Z. (1977). The nervous system of Loligo, III. Higher motor centres: the basal supraoesophageal
474 lobes. Philosophical Transactions of the Royal Society of London. B, Biological Sciences, 276(948), 351-
475 398. https://royalsocietypublishing.org/doi/abs/10.1098/rstb.1977.0003
476 Young, J. Z. (1979). The nervous system of Loligo. V. The vertical lobe complex. Philosophical
477 Transactions of the Royal Society of London. B, Biological Sciences, 285(1009), 311-354.
478 https://royalsocietypublishing.org/doi/abs/10.1098/rstb.1979.0008
479 Zullo, L., Sumbre, G., Agnisola, C., Flash, T., & Hochner, B. (2009). Nonsomatotopic organization of the
480 higher motor centers in octopus. Curr Biol, 19, 1632-1636. https://doi.org/10.1016/j.cub.2009.07.067

Brain region	Abbreviation	Function
Supraesophageal mass		
Vertical lobe complex		**Learning and memory (Young, 1991)**
Vertical lobe	V	
Subvertical lobe	SV	
Superior frontal lobe	SF	
Inferior frontal lobe	IF	
Posterior frontal lobe	PF	
Basal lobe complex		**Higher motor control (Boycott, 1961)**
Anterior anterior basal lobe	AAB	Movement of head, arms and eyes
Anterior posterior basal lobe	APB	
Precommissural lobe	PC	
Dorsal basal lobe	DB	
Interbasal lobes	IB	Movement of feeding tentacles
Median basal lobe	MB	Movement of mantle and funnel during swimming and breathing; protraction and retraction of head; movement of fins, movement of buccal mass, and expansion and contraction of chromatophores
Lateral basal lobes	LB	Control of chromatophores and papillae
Subesophageal mass		
Pedal lobe complex		**Intermediate and lower motor control of movement (Boycott, 1961)**
Anterior pedal lobe	AP	Movement of arms and tentacles
Posterior pedal lobe	PP	Movement of funnel, fins and tentacles; head retraction
Lateral pedal lobes	LP	Movement of eyes
Anterior dorsal chromatophore lobes	ADC	Control of chromatophores and papillae on the head and arms
Anterior ventral chromatophore lobes	AVC	Control of chromatophores and papillae on the head and arms
Magnocellular lobe complex		**Giant fiber response (escape movements) (Boycott, 1961)**
Dorsal magnocellular lobes	DM	
Ventral magnocellular lobes	VM	
Posterior magnocellular lobes	PM	
Palliovisceral lobe complex		**Lower motor control of locomotion (Boycott, 1961)**
Palliovisceral lobe	PV	Control of escape movements and ink ejection
Lateral ventral palliovisceral lobes	LPV	
Fin lobes	F	Movement of fins
Posterior chromatophore lobes	PC	Control of chromatophores and papillae on mantle, fin and visceral mass
Dorsal vasomotor lobe	DV	
Ventral vasomotor lobe	VV	
Brachial lobe complex		**Motor control of arms and feeding**
Brachial lobe	B	Intermediate motor control of arms
Superior buccal lobe	SB	Biting movements of the buccal mass
Inferior buccal lobe	IB	Biting movements of the buccal mass
Periesophageal mass		
Optic-tract complex		
Optic lobes	O	Visual processing (Boycott, 1961)
Peduncle lobes	P	Visuo-motor control (Messenger, 1967)
Dorsolateral lobes	DL	
Optic glands	OG	Neurosecretory center (Messenger, 1967)
Olfactory lobes	OL	Unclear (Messenger, 1979)
Nerve fibers		
Ventral optic commissure	VOC	
Optic to anterior basal lobe tracts	OAB	
Subvertical to optic tracts	SOT	
Lateral basal to posterior chromatophore lobe tracts	LBPC	
Brachio-palliovisceral connectives	BPC	
Anterior magnocellular commissure	AMC	
Pallial nerves	PN	
Optic to vertical lobe tracts	OV	
Optic to dorsal magnocellular lobe tracts	ODM	

Table 1. The lobes of the cuttlefish brain.

Abbreviation	Brain lobe	Number of voxels	Volume mm^3	Proportion of the brain	
Ol	optic	923066	115.3832552	36.79%	
Or		942863	117.8578803	37.57%	**74.36%**
Pl	peduncle	6915	0.864375039	0.28%	
Pr		6869	0.858625038	0.27%	**0.55%**
OLl	olfactory	1122	0.140250006	0.04%	
OLr		927	0.115875005	0.04%	**0.08%**
DLl	dorsolateral	1738	0.21725001	0.07%	
DLr		1814	0.22675001	0.07%	**0.14%**
SV	subvertical	36379	4.547375203	1.45%	**1.45%**
V	vertical	128404	16.05050072	5.12%	**5.12%**
PC	precommissural	12129	1.516125068	0.48%	**0.48%**
MB	median basal	16639	2.079875093	0.66%	**0.66%**
DB	dorsal basal	43502	5.437750243	1.73%	**1.73%**
LBl	lateral basal	4871	0.608875027	0.19%	
LBr		4953	0.619125028	0.20%	**0.39%**
IBl	interbasal	1138	0.142250006	0.05%	
IBr		1550	0.193750009	0.06%	**0.11%**
SF	superior frontal	26603	3.325375149	1.06%	**1.06%**
IF	inferior frontal	5391	0.67387503	0.21%	**0.21%**
PF	posterior frontal	5116	0.639500029	0.20%	**0.20%**
AAB	anterior anterior basal	20829	2.603625116	0.83%	**0.83%**
APB	anterior posterior basal	12924	1.615500072	0.52%	**0.52%**
DMl	dorsal magnocellular	13652	1.706500076	0.54%	
DMr		14622	1.827750082	0.58%	**1.13%**
VMl	ventral magnocellular	2850	0.356250016	0.11%	
VMr		2702	0.337750015	0.11%	**0.22%**
PMl	posterior magnocellular	7179	0.89737504	0.29%	
PMr		7338	0.917250041	0.29%	**0.58%**
B	brachial	45948	5.743500257	1.83%	**1.83%**
ADCl	anterior dorsal chromatophore	790	0.098750004	0.03%	
ADCr		747	0.093375004	0.03%	**0.06%**
AVCl	anterior ventral chromatophore	971	0.121375005	0.04%	
AVCr		934	0.116750005	0.04%	**0.08%**
PCl	posterior chromatophore	3723	0.465375021	0.15%	
PCr		4196	0.524500023	0.17%	**0.32%**
AP	anterior pedal	31888	3.986000178	1.27%	**1.27%**
PP	posterior pedal	30382	3.79775017	1.21%	**1.21%**
LPl	lateral pedal	7817	0.977125044	0.31%	
LPr		8302	1.037750046	0.33%	**0.64%**
PV	palliovisceral	27149	3.393625152	1.08%	**1.08%**
LPVl	lateral palliovisceral	5252	0.656500029	0.21%	
LPVr		4226	0.528250024	0.17%	**0.38%**
Fl	fin	11736	1.467000066	0.47%	
Fr		11120	1.390000062	0.44%	**0.91%**
OGl	optic gland	434	0.054250002	0.02%	
OGr		744	0.093000004	0.03%	**0.05%**
VV	ventral vasomotor	3946	0.493250022	0.16%	**0.16%**
DV	dorsal vasomotor	6353	0.794125036	0.25%	**0.25%**
VOC	ventral optic commissure	4721	0.590125026	0.19%	**0.19%**
LBPCl	lateral basal to posterior chromatophore tract	807	0.100875005	0.03%	
LBPCr		897	0.112125005	0.04%	**0.07%**
BPCl	brachio-palliovisceral connective	2908	0.363500016	0.12%	
BPCr		3143	0.392875018	0.13%	**0.24%**
PNl	pallial nerve	2437	0.304625014	0.10%	
PNr		2324	0.290500013	0.09%	**0.19%**
AMC	anterior magnocellular commissure	1852	0.23150001	0.07%	**0.07%**
SOTl	subvertical to optic tracts	964	0.120500005	0.04%	
SOTr		660	0.082500004	0.03%	**0.06%**
OABl	optic to anterior basal lobe tract	5414	0.67675003	0.22%	
OABr		4805	0.600625027	0.19%	**0.41%**
OVl	optic to vertical lobe tract	7072	0.88400004	0.28%	
OVr		8156	1.019500046	0.33%	**0.61%**
ODMl	optic to dorsal magnocellular lobe tract	1259	0.157375007	0.05%	
ODMr		1174	0.146750007	0.05%	**0.10%**
Entire brain		**2509336**	**313.667014**	100.00%	100.00%

Table 2. Volume of cuttlefish brain lobes

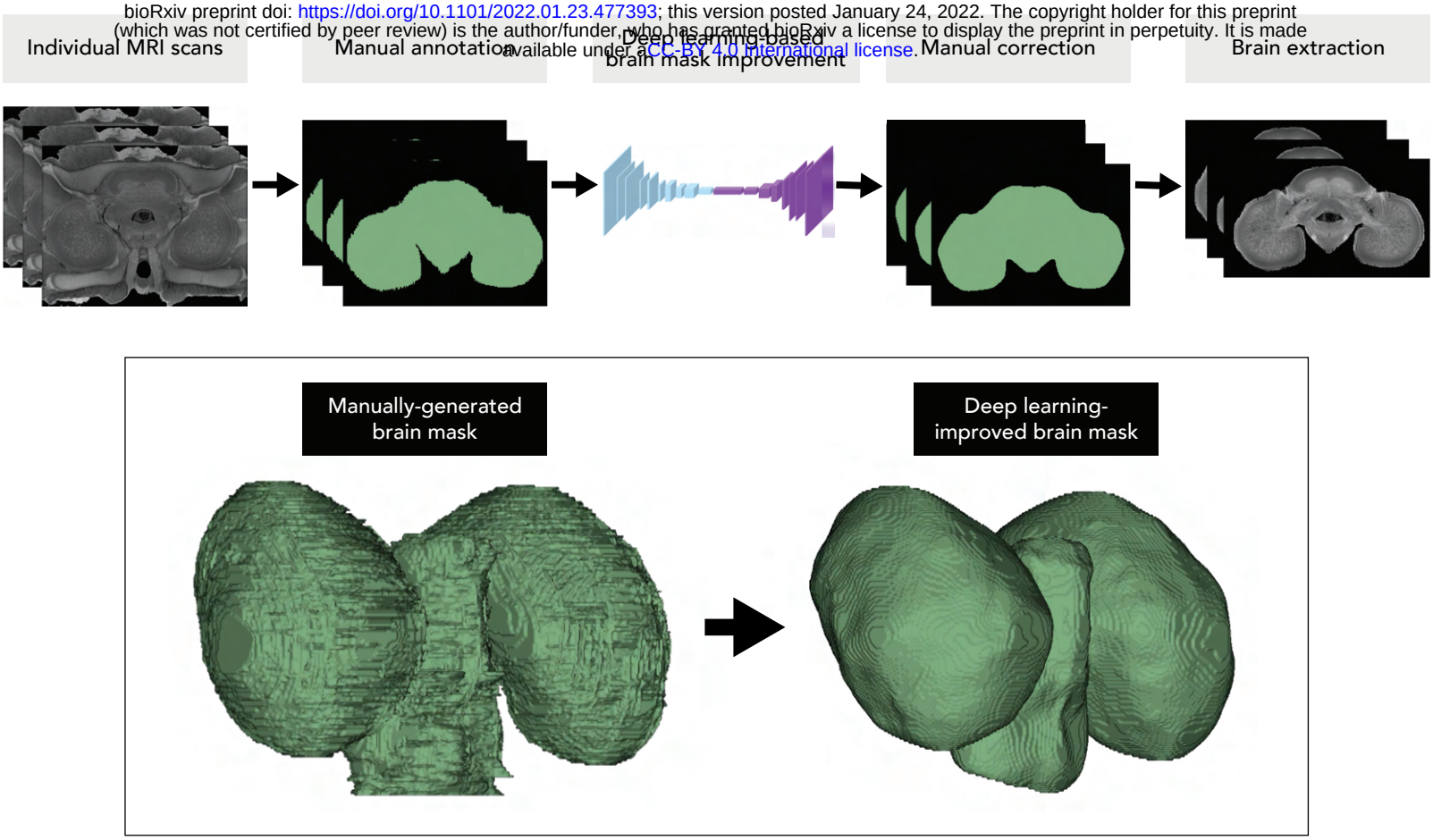

Figure S1. Deep learning pipeline for improving manually-generated brain masks.